Multiscale Water Dynamics on Protein Surfaces: Protein-Specific Response to Surface Ions

Tadeja Janc, Jean-Pierre Korb, Miha Lukšič, Vojko Vlachy, Robert G Bryant, Guillaume Mériguet, Natalie Malikova, Anne-Laure Rollet

Multi-scale Water Dynamics on Protein Surfaces: Protein-specific Response to Surface Ions

Journal:	*The Journal of Physical Chemistry*
Manuscript ID	jp-2021-02513t.R2
Manuscript Type:	Article
Date Submitted by the Author:	n/a
Complete List of Authors:	Janc, Tadeja; University of Ljubljana, Faculty of Chemistry and Chemical Technology Korb, Jean-Pierre; Sorbonne-Universite-CNRS, Phenix Laboratory Luksic, Miha; Univerza v Ljubljani, Faculty of chemistry and chemical technology Vlachy, Vojko; University of Ljubljana, Faculty of Chemistry and Chemical Technology Bryant, Robert; University of Virginia, Chemistry Department Mériguet, Guillaume; Sorbonne University, Lab PHENIX Malikova, Natalie; UPMC, PHENIX Rollet, Anne-Laure; CNRS, PHENIX

Multi-scale Water Dynamics on Protein Surfaces: Protein-specific Response to Surface Ions

Tadeja Janc,[†,‡] Jean-Pierre Korb,[†] Miha Lukšič,[‡] Vojko Vlachy,[‡] Robert G. Bryant,[¶] Guillaume Mériguet,[†] Natalie Malikova,[*,†] and Anne-Laure Rollet[†]

†*Laboratoire PHENIX, CNRS, Sorbonne Université, Paris, France*

‡*Faculty of Chemistry and Chemical Technology, University of Ljubljana, 1000 Ljubljana, Slovenia*

¶*Chemistry Department, University of Virginia, Charlottesville, Virginia 22904, United States*

E-mail: natalie.malikova@sorbonne-universite.fr

Abstract

Proteins function in crowded aqueous environments interacting with a diverse range of compounds, among them dissolved ions. These interactions are water mediated. In the present study we combine field dependent NMR relaxation (NMRD) and theory to probe water dynamics at the surface of protein in concentrated aqueous solutions of hen egg-white lysozyme (LZM) and bovine serum albumin (BSA). The experiments reveal that presence of salts (NaCl or NaI) leads to an opposite ion-specific response for the two proteins: an addition of salt to LZM solutions increases water relaxation rates with respect to the salt-free case, while for BSA solutions a decrease is observed. The magnitude of the change depends on the ion identity. The developed model accounts for the non-Lorentzian shape of the NMRD profiles and reproduces the experimental data over four decades in Larmor frequency (10 kHz to 110 MHz). It is applicable

up to high protein concentrations. The model incorporates the observed ion-specific effects via changes in the protein surface roughness, represented by the surface fractal dimension, and the accompanying changes in the surface water residence times. The response is protein-specific, linked to geometrical aspects of the individual protein surfaces, and goes beyond protein-independent Hofmeister-style ordering of ions.

Introduction

Interactions between protein macromolecules are at the heart of the many biochemical processes in the cell. Protein-protein interaction affects their phase behavior: aggregation, liquid-liquid phase separation, and possible crystallization.[1–3] Protein aggregation in the living cell may lead to Alzheimer's disease, cataracts of eye lenses, etc.[4] while delivery of an unstable protein-based drug may cause health complications.[5] To mimic natural environments and drug formulations, proteins need to be considered at relatively high concentrations, of the order of 100 mg/mL, and in buffer-saline media.[6–8] In such systems proteins interact with water, buffer ions, salt ions, as also with other additives (sugars, polymers etc.). The chemical nature of the low molecular mass salts, such as, NaCl, NaI, or others is important: salts affect the stability of aqueous protein solutions differently. The ranking of salt-specific or ion-specific effects, known also as the Hofmeister series, depends on the type of the protein (or other kind of macromolecule/colloid), experimental conditions, as well as the measured property.[9–15]

The protein-ion and consequently also the protein-protein interactions are water-mediated, so knowing the status of intervening water molecules is important. The many processes taking place on the protein surface involve hydration and de-hydration of ions and/or charged groups. Surface water and ions radically influence the restructuring of the protein itself, which is known to have large-scale structural fluctuations on remarkably short time scales.[16] The energies holding a particular fold are small even for maintaining a defined structure. The stability may be only 5-8 kcal/mol which is only an order of magnitude larger than

the thermal fluctuation at room temperature, $RT \approx 0.5$ kcal/mol. Overall, water molecules transiently bound to the surface and incorporated into the core of protein molecules play a critical role in biological functions of these proteins.[17] The central question of the present study is how the dynamics of these water molecules is influenced by ions at different positions along the Hofmeister series, and this up to the concentrated protein state, mimicking real conditions of interest.

Field-dependent NMR relaxation or NMRD[18] is a technique offering unique opportunities for characterizing the multi-scale dynamics of NMR-active nuclei, which for biological systems concern most widely the ^{1}H (proton) nuclei, but also ^{2}H and ^{17}O and other nuclei.[19,20] NMRD measurements have been employed with a considerable success to study the dynamics of structural protons of the protein, e.g.,[21,22] the overall tumbling motion of the protein, e.g.,[23,24] and the dynamics of water molecules associated with the protein surface and its cavities.[19,25–28] We focus on the latter here.

The NMRD technique involves varying the magnetic field strength (Larmor frequency) to explore the correlation times for ^{1}H dipole-dipole fluctuations that drive the nuclear spin relaxation. This leads to a description of water dynamics at the protein surface over multiple time scales, ranging from ps to μs.[19,20,28] NMRD experiments allow distinguishing water molecules as a function of their residence time on the protein surface.[29] In the low-frequency range, from 10 kHz to 10 MHz, slow water motion dictates the NMR relaxation. These are caused by only a few water molecules trapped in potential energy wells on the protein surface and thus a long residence time on the protein surface. Due to such trapping, their rotational correlation time is the same as that of the protein, of the order of several tens of ns. The effect of such embedded water molecules has been extensively studied in the past, for the cases of freely rotating proteins in solution as well as immobilized proteins.[19,20,25,26,30,31] In the high frequency range, between 20 and 300 MHz, fast water motion dominates. The contribution to NMR relaxation here is dominated by water molecules moving (or jumping) on the protein surface, with rotational correlation times of the order of several ps.[27,28,32] After

some time spent next to the protein surface they may diffuse away and join bulk water. Such water molecules are in contact with the surface for much shorter times, they are not trapped or localized.

So-far, effects of salt ions on surface water dynamics, seen on ^{1}H NMRD profiles as a drastic increase in the water relaxation rates in the low frequency range, have been interpreted by evoking the formation of protein oligomers.[33,34] We shall see that for low salt concentrations considered here, salt ions can lead to both an increase or a decrease in the NMR relaxation rates, depending on the type of the protein. Further, the magnitude of such increase or decrease depends on the position of the ion in the Hofmeister series. The aforementioned interpretation (oligomer formation) cannot be used to rationalise the trends observed and an alternative is developed here. The core of the proposed model lies in the modification of access to water surface sites, for both the embedded and surface water molecules. The model successfully reproduces the experimental NMRD relaxation profiles over four decades in the Larmor frequency, from 10 kHz to 110 MHz.

Materials and Methods

Hen egg-white lysozyme (LZM, $M_w \approx 14.3$ kDa) was purchased from Merck Milipore (lot number: K46535581 514), and bovine serum albumin (BSA, free of fatty acids, purity $\geq$ 96%, $M_w \approx 66.5$ kDa) was purchased from Sigma Aldrich (lot number: SLBM9552V). 100% acetic acid, 1 M NaOH, NaCl, and NaI were supplied by Merck. All solutions were prepared with Milli Q water and filtered through 0.45 μm Minisart Sartorious filters. Buffer (CH_3COONa/CH_3COOH) concentration was 20 mM with a pH value of 4.0. Protein powder was diluted in acetate buffer and dialyzed against the same buffer which was replaced by a fresh one three times in 24 hours. Dialysis cassettes with M_w cutoff 3.5 kDa were used. After dialysis protein solutions were concentrated with spin column concentrators with M_w cutoff 10 kDa for LZM and 50 kDa for BSA. The measured pH for 160 mg/mL of LZM

solution in 20 mM acetic buffer was 4.2 while for BSA it was 4.1. The concentration of both proteins was determined by UV-vis spectrophotometer (Varian Cary 100 Bio) at 280 nm where extinction coefficient for LZM is 2.635 mL mg^{-1} cm^{-1} [35] and for BSA 0.667 mL mg^{-1} cm^{-1}.[36] Protein-buffer and salt-buffer solutions were mixed together in the desired ratio just before each measurement.

Longitudinal NMR relaxation measurements

Longitudinal relaxation time, T_1 ($T_1 = 1/R_1$), was measured by two NMR relaxometers. The temperature inside the probe was set at 30 °C. Relaxation between 10 kHz and 30 MHz (of ^{1}H Larmor frequency) was measured by Spinmaster FFC2000 1T C/DC, Stelar (fast field cycling relaxometer). 10 mm diameter NMR tubes were filled with 1.2 mL of sample volume. For frequency range between 12 MHz and 30 MHz non-polarized (NP) sequence was employed while below 12 MHz spins were pre-polarized for 2 s by the magnetic field (B_p) of 20 MHz. Free-induction decay (FID) followed by a single 90° excitation pulse (≈ 9 μs) was recorded at 16.3 MHz (B_acq). The switching time between different frequencies was 3 ms. Around 64 logarithmically spaced increments were measured to determine T_1 with the maximum value of 1 s and relaxation delay of 10 s. At higher frequency range i.e. between 30 MHz and 110 MHz High field NMR relaxometer (3T), Stelar was employed. 5 mm diameter NMR tubes were used with only 60 μL of sample volume. In the inversion-recovery pulse sequence recycle delay was set to 10–15 s, while 16 exponential increments were measured with T_1 maximum value of 2.5 s.

Results

Experimental signature of ion-specific effects on protein surface by NMRD

The effects of added NaCl and NaI salts were studied in LZM and BSA buffer solutions (20 mM CH_3COONa/CH_3COOH, pH = 4.0) at T = 30 °C. The isoionic point is ≈ 11.2 for LZM and ≈ 4.7 for BSA. Under the pH studied, both proteins possess an overall positive charge and thus our interest focused on studying a sequence of salts with different anions, for a common cation. The protein concentration was 160 mg mL^{-1}. NMRD measurements of the longitudinal relaxation rate, R_1, were performed at ^{1}H Larmor frequencies between 10 kHz and 110 MHz. Mono-exponential magnetization recovery curves were observed in these measurements and the R_1 values result from mono-exponential fitting of these curves.

Figure 1 shows the principal result of this study. It presents ^{1}H NMRD R_1 profiles for LZM (top) and BSA (bottom) solutions. For LZM R_1 increases after salt addition (No salt < (0.05 M) NaCl < (0.05 M) NaI) but for BSA the order is reversed (No salt > (0.10 M) NaCl > (0.10 M) NaI). Clearly, the influence of the added salt is more pronounced at lower frequencies, though still visible at higher frequencies, e.g. 20 MHz, where typical NMR relaxation experiments are carried out. The length of diffusion, l_D, sensed during an NMR experiment depends on the Larmor frequency:

$l_D(\omega_0) \approx \sqrt{6D_{diff}/\omega_0}$, where D_{diff} is the three-dimensional diffusion coefficient of the proton-bearing species.[28] In other words, the R_1 signal detected at lower frequencies is associated with a much larger diffusion length of the ^{1}H nuclei, which have time to explore an increasingly richer set of environments. The data in Figure 1 are clearly consistent with our previous measurements at a single frequency of 20 MHz, which showed an increased sensitivity of R_2 (transverse NMR relaxation rate), as opposed to R_1, to the salt specific effects in LZM and BSA solutions.[37] R_2 measurements, contrary to R_1, contain the zero-frequency spectral component probing the slow (low-frequency) relaxation processes.[18,28]

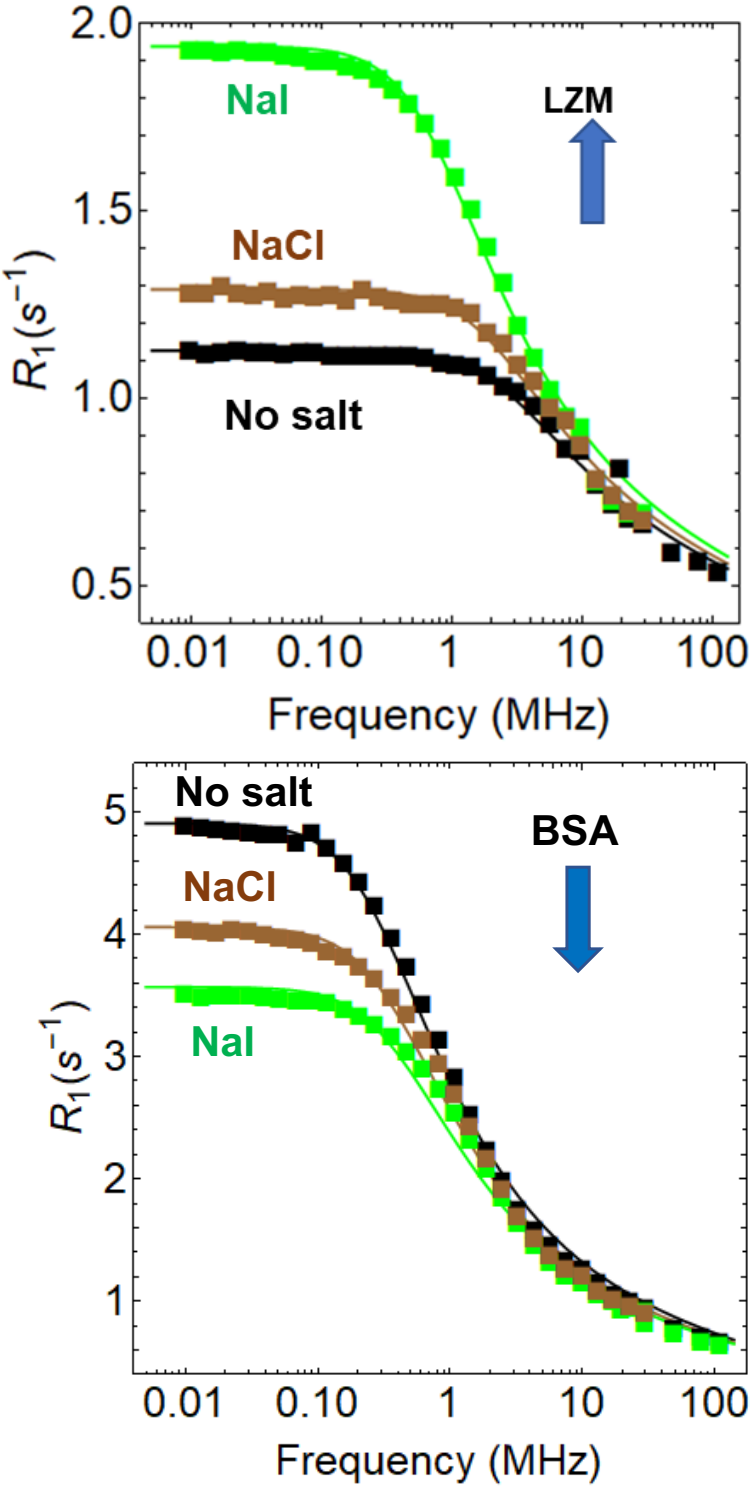

Figure 1: ^{1}H NMRD R_1 profiles for LZM (top) and BSA (bottom) solutions as a function of ^{1}H Larmor frequencies between 10 kHz and 110 MHz. Salt addition causes an increases of the R_1 relaxation rate for LZM and a decrease for BSA (arrows). Symbols represent measurements while the continuous lines represent our theoretical model (Equation 26-SI; fitting parameters in Table 1). T = 30 °C and c_m=160 mg/mL, 20 mM CH_3COONa / CH_3COOH, pH = 4.0, c_{salt}=0.05 M for LZM and 0.1 M for BSA.

Importantly, the current multi-frequency data incite the development and allow the testing of a multi-scale model of the water dynamics at protein surfaces, in order to explain the protein-specific response in Figure 1. The model considers both long-lived ("embedded") and short-lived ("transiently diffusing") water molecules on the protein surface. Currently, the model does not consider a contribution from proton-exchange between labile protons of protein surface groups and water molecules. The justification lies in the very weak temperature dependence of the observed NMRD profiles. This is shown in Figure 1 of SI, where $R_1(20\ ^\circ\mathrm{C})/R_1(30\ ^\circ\mathrm{C}) \approx 1.2$, which is inconsistent with an activated process of proton exchange, with a typical activation energy of 25 kJ/mol. Furthermore, the internal protein structure was checked by circular dichroism and confirms that no changes in the secondary structure of the two proteins take place in the presence of the salts considered here.

Multi-scale model of water dynamics on protein surface

Our NMRD experiments show an interesting phenomenon of salt effect reversal on the R_1 NMRD profiles, depending on the nature of the protein. In this section we shall develop a model that accounts for these changes and provides information, over a wide frequency range, about relaxation of water protons present transiently at the protein surface. The starting point for the modelling of R_1 profiles in NMRD is a Lorentzian function. Departures from the single Lorentzian behaviour are however very common, the general solution being the superposition of several (2-3) Lorentzian contributions.[20,22,33,34,38,39] In our case, the use of a single Lorentzian fails as it corresponds to a steep dependence at intermediate frequencies and a high-frequency plateau. Both of these features are inconsistent with the experimental curves in Figure 1. Further, as mentioned previously, a sum of Lorentzian contributions cannot provide an explanation for the observed salt effects, especially the *decrease* of the low-frequency R_1 plateau. These reasons encouraged us to propose a different theoretical interpretation of the NMRD profiles for protein solutions.

$R_1(\omega_0)$ profiles are modelled by a sum of contributions from the "embedded" and "sur-

face" water molecules, represented respectively by a *slow* and *fast* surface relaxation process. To account for relaxation rates over a large protein concentration range, reaching up to high concentrations (160 mg mL^{-1} for data in Figure 1), we considered the inter-protein distances with respect to the size of individual protein molecules (see SI p. 1). For high protein concentrations, where the inter-protein distance is similar or even smaller than protein size, it is necessary to introduce the notion of ^{1}H nuclei of water exploring not only a single protein surface ("single surface exploration" or "sse"), but also several protein surfaces ("double surface exploration" or "dse"). The general expression we employ for $R_1(\omega_0)$ thus becomes

$$R_1(\omega_0) = R_1^{\mathrm{bulk}} + \sum_{\mathrm{i=sse,dse}} \frac{N_{\mathrm{surf}}^{\mathrm{i}}}{N} \left[R_{1,\mathrm{slow}}^{\mathrm{surf,i}}(\omega_0) + R_{1,\mathrm{fast}}^{\mathrm{surf,i}}(\omega_0) \right] \quad (1)$$

where $\omega_0/2\pi$ is the ^{1}H Larmor frequency and R_1^{bulk} is the relaxation rate of bulk water which has no frequency dependence in the frequency range studied.

For each *slow* and *fast* surface relaxation process, the relaxation rate $R_1^{\mathrm{surf}}(\omega_0)$ can be expressed as a linear combination of the corresponding spectral density, $J^{\mathrm{surf}}(\omega_0)$ [18,28]

$$R_{1,\mathrm{x}}^{\mathrm{surf}}(\omega_0) = B_{\mathrm{x}} \left[J_{\mathrm{x}}^{\mathrm{surf}}(\omega_0) + 4J_{\mathrm{x}}^{\mathrm{surf}}(2\omega_0) \right] \quad (2)$$

where x corresponds to either "slow" or "fast". The first important step is now to identify and adapt existing expressions for $J_{\mathrm{fast}}^{\mathrm{surf}}(\omega_0)$, B_{fast} and their analogues $J_{\mathrm{slow}}^{\mathrm{surf}}(\omega_0)$, B_{slow}. This shall be done on the basis of previously published models of Korb *et al.*[31] and Grebenkov *et al.*[27] for the slow and fast surface relaxation processes respectively. The second crucial step will be the evaluation of the relative intensities of the different contributions in Equation 1, i.e. the pre-factors $N_{\mathrm{surf}}^{\mathrm{i}}/N$, which are the fractions of water molecules being transiently present at the protein surface and taking part in one of the surface relaxation processes. This term will be seen to depend on the roughness of the protein surface and it is a key to

our explanation of the different salt-specific effects observed here for LZM and BSA.

Slow surface relaxation: water in potential energy wells on the protein surface

As mentioned previously, the very long timescales (order of several μs) explored in the low frequency range (below 10 MHz) allow to observe the rare escape events from the binding sites of water molecules most strongly held or "embedded" in the potential energy landscape of the protein surface. The expression we use for $R_{\rm slow}^{\rm surf}(\omega_0)$, see SI p. 2, is inspired by the one introduced for water dynamics (heavy and light water) at the surface of cross-linked protein gels.[31] To arrive at the expression for $R_{\rm slow}^{\rm surf}(\omega_0)$ (see Equations 8-SI to 10-SI), the theory of the extreme value statistics of rare events was applied. From a mathematical point of view, we consider the possibility that "embedded" water molecules make rare transitions between two local and unequal wells characterized by different activation energies: $E' < E$ (see Figure 3-SI). In such cases, a water molecule experiences two environments that may be characterized by different magnitudes of dipolar coupling constants, $\omega_{d1} < \omega_{d2}$ and it contributes to relaxation only if it exchanges with another water molecule trapped in a neighbouring well with a different depth. Such modelling of water binding sites leads to a large distribution of waiting times needed for a water molecule to change wells, i.e. $\tau_{\rm min} \leq \tau \leq \tau_{\rm max}$ with $\tau_{\rm min} \ll \tau_{\rm max}$. The distribution has a Pareto form, it is characterised by the Pareto exponent $\alpha = \frac{k_b T}{E(T) - E'(T)} = \frac{k_b T}{\Delta E(T)}$ and describes the waiting time needed for a water molecule to jump between the two wells. The two wells are assigned activation energies $E' = E_{\rm d} + E'_{\rm A}$ and $E = E_{\rm d} + E_{\rm A}$, where $E_{\rm d} = 4.7$ kcal/mol is the diffusion barrier for unbound water, and $E_{\rm A}$ and $E'_{\rm A}$ correspond to the depths of the two successive wells. To evaluate $R_{\rm slow}^{\rm surf}(\omega_0)$, the spectral density function, $J_{\rm slow}^{\rm surf}(\omega_0)$, has to be averaged over two normalized Pareto distribution functions, each corresponding to the two wells involved in the exchange. Overall, the two parameters that we shall extract from the fitting of the slow relaxation process is the upper bound of the energy well depth, $E'_{\rm A,max}$, and the corresponding upper bound of the waiting time, $\tau'_{\rm max}$.

Fast surface relaxation: transient water diffusion on the protein surface

In the intermediate frequency range ($30 \leq \omega_0/2\pi \leq 110$ MHz), the source of relaxation comes from the dipole-dipole interaction between the ^{1}H nuclei of the protein and those from water molecules diffusing transiently on the surface of protein. These are fast motions and we use a theoretical interpretation of $R^{\text{surf}}_{1,\text{fast}}(\omega_0)$ at this frequency range proposed by Grebenkov *et al.*,[27] see SI p. 4.

The expression for $R^{\text{surf}}_{1,\text{fast}}(\omega_0)$, see Equations 12-SI to 14-SI introduces two correlation times of water molecules: τ_s and τ_m. $\tau_m \approx 37$ ps and characterizes surface correlation times of water at the protein surface that is inversely proportional to the surface translational coefficient $D_{\text{surf}}/D_{\text{bulk}} = 1/3$.[27] τ_s ($\gg \tau_m$) is the time of water residence at the protein surface. The ratio τ_s/τ_m corresponds to the average number of molecular steps or jumps on the protein surface, it is also called the dynamical surface affinity or NMR wettability, A,[28] and it is the parameter we extract from the the fitting of the fast relaxation process.

Water fraction at the protein surface, "single" versus "double" surface exploration

In this section, we are concerned with developing an expression for the fractions of water molecules present transiently at the protein surface, involved in the "single surface exploration" or "double surface exploration". These are the $N^{\text{i}}_{\text{surf}}/N$ pre-factors in Equation 1. As a point of departure, the total fraction of surface water molecules can be formally expressed as

$$\frac{N_{\text{surf}}}{N} = \frac{\varepsilon S_{\text{T}}}{V_{\text{T}}} = \frac{\varepsilon c_m N_{\text{A}} S_1}{M_{\text{w}}}, \tag{3}$$

where $\varepsilon \approx 3$ Å represents the thickness of a single layer of water molecules transiently situated on the protein surface; S_{T} and V_{T} are respectively the total protein surface and the total volume of the system; M_{w} is the protein molecular mass (≈ 14.3 kDa for LZM and ≈ 66.5

kDa for BSA), c_m the protein mass concentration, N_A the Avogadro's number and S_1 surface of a single protein molecule.

In the first modification to Equation 3 we introduce the protein surface roughness, as a critical parameter influencing S_1. We consider that the protein surface roughness depends initially on the protein identity (BSA or LZM), but is modulated further by the adsorption of ions at the protein surface. Crucially, this modulation can act either way, to decrease or to increase the total accessible protein surface, depending on the initial roughness, as depicted schematically in Figure 2. This is a central idea evoked to explain the opposite trends observed for $R_1(\omega_0)$ on salt addition for BSA and LZM solutions.

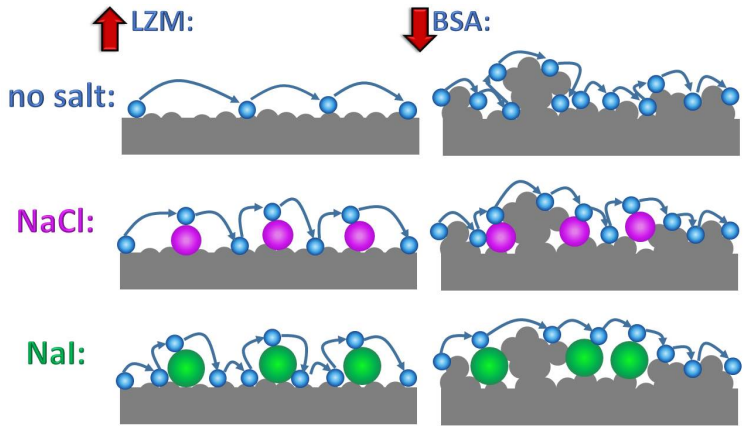

Figure 2: Schematic representation of salt-specific effects on protein surfaces - LZM (left) and BSA (right). Blue spheres represent water molecules, while magenta and green spheres are Cl^- and I^- ions, respectively. Red arrows indicate the changes in the surface roughness experienced by water molecules transiently present at each of the protein surfaces: for LZM surface roughness increases along the sequence No salt $\rightarrow$ NaCl $\rightarrow$ NaI (from top to bottom), while for BSA surface roughness decreases along this sequence.

To estimate the solvent accessible area, we expressed protein surface roughness using a scaling approach considering a geometrical series over a hierarchy in the number N^n of different proton-containing species (proteins, hydrated ions and water molecules) labeled by an integer index n with $0 \leq n \leq K = 2$ (see SI p. 4). The size of the proton-containing spherical species in the category n is decreasing as R_0/β^n, where $\beta = 5$ and R_0 is the protein radius of gyration. We introduce the hierarchy with the relation, $N^n \propto \beta^{d_f}$, where $2 \leq d_f \leq 3$ is the surface fractal dimension. The total surface of a single hydrated spherical protein (S_1)

calculated up to a category $K = 2$ thus becomes a geometrical series, see Equation 15-SI. This approach allows to express protein roughness with a single parameter, i.e. the surface fractal dimension d_f. Higher d_f indicates a rougher surface, thus higher N_surf/N and consequently higher values for $R_1(\omega_0)$.

In the second modification to Equation 3 we consider the possibility of "double protein surface exploration" for a given fraction of water molecules. This is a consequence of a close approach of individual protein surfaces, as the protein concentration increases. In Figure 2-SI the dependence of an average inter-protein distance, $\langle d \rangle$, on protein concentration, c_m, is displayed. $\langle d \rangle$ varies between 100-150 Å at the lowest concentration (10 mg mL^{-1}) down to 20 Å in the high concentration limit (160 mg mL^{-1}). In this limit $\langle d \rangle$ is very close to the protein radii of gyration ($\approx$ 15.0 Å for LZM[40] and $\approx$ 34.8 Å for BSA[41]). Thus we propose a scenario where, at high protein concentrations, water molecules can explore, on the time-scale of the NMRD experiment, not just a single protein surface, but also that of its neighbour, we shall refer to this as "double surface exploration", as opposed to "single surface exploration". In the following these two situations are referred to by the D and S symbols respectively. The principal idea behind estimating the fraction of water molecules involved in the "double surface exploration" is to borrow the concept of equilibrium between two states, "single" and "double", represented by $S + S \rightleftharpoons D$. For such a situation we can define an equilibrium constant, K_eq, as well as equilibrium concentrations $[S]$ and $[D]$. This leads to the following expressions for the water surface fractions N_surf/N for the case of "single" and "double" surface exploration (for more details see SI p. 5):

$$\left(\frac{N_\mathrm{surf}}{N}\right)_\mathrm{sse} = \frac{1}{4K_\mathrm{eq}}\left[-1 + \sqrt{1 + 8K_\mathrm{eq}\frac{c_m}{M_\mathrm{w}}}\right]\varepsilon N_\mathrm{A} S_1 \tag{4a}$$

$$\left(\frac{N_\mathrm{surf}}{N}\right)_\mathrm{dse} = \frac{1}{8K_\mathrm{eq}}\left[1 + 4K_\mathrm{eq}\frac{c_m}{M_\mathrm{w}} - \sqrt{1 + 8K_\mathrm{eq}\frac{c_m}{M_\mathrm{w}}}\right]\varepsilon N_\mathrm{A} S_1 \tag{4b}$$

We are aware that there is a difference between dividing the population of water molecules into the "single" and "double surface explorers" on one hand and dividing the *proteins* into

two categories (those explored as a single surface and those as part of a double surface) on the other hand. It is the latter scenario that is depicted by the above equilibrium concept. We consider however that in a first approach this is a plausible and promising way to tackle the problem. In Figure 3 we combine the effects of surface roughness and single/double

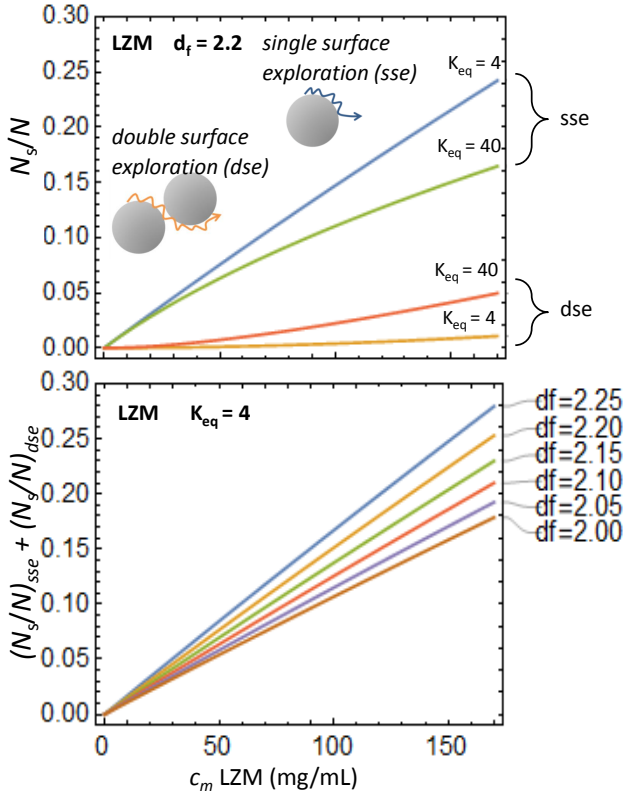

Figure 3: Upper panel: Contributions of single and double surface explorers to N_{surf}/N for LZM solution considering a fixed surface roughness ($d_{\mathrm{f}} = 2.2$) and for two equilibrium constants (K_{eq} of 4 and 40). The schematic inserts show single and double surface explorers. Lower panel: The sum of single and double surface explorers for different values of protein surface roughness (d_{f}) for the case of LZM. The curves have been obtained from Eqs. (4 and 15-SI) varying the protein concentrations, c_{m}.

surface exploration to calculate N_{surf}/N and its different contributions for LZM protein, for a large protein concentration range. The total surface of a single hydrated protein, S_1, (Eq. 15-SI) is expressed in terms of d_{f}. Eqs. 16-SI and 17-SI show the dependence of $(N_{\mathrm{s}}/N)_{\mathrm{sse}}$ and $(N_{\mathrm{s}}/N)_{\mathrm{dse}}$ on S_1 and consequently, on d_{f}. Two observations regarding Figure 3 are important: (i) The single contribution has a close to linear dependence on c_m, while

the double contribution is quadratic in c_m but remains weak except at large c_m and for large values of $K_{\rm eq}$. However, the nonlinear effect of the double contribution will enhance $R_1(\omega_0)$ significantly, as the corresponding correlation times are higher than for the single contribution. (ii) The influence of $d_{\rm f}$ grows with increasing protein concentration.

Overall shape and modelling of $R_1(\omega_0)$

The general shape of $R_1(\omega_0)$ can be summarized as follows: $R_1(\omega_0)$ approaches a constant value when $\omega_0 \to 0$, at intermediate frequencies it decays as a sum of a power law (signature of the $R^{\rm surf}_{\rm slow}(\omega_0)$ component) and at large frequencies shows a logarithmic law (signature of the $R^{\rm surf}_{\rm fast}(\omega_0)$ component). In Figure 6-SI, we show the decoupling of the overall signal into the individual contributions. In Figure 1 we display the best fits of $R_1(\omega_0)$, with the overall expression for $R_1(\omega_0)$ as shown by Equation 26-SI.

Slow surface relaxation modelling: (i) The fixed parameters are: $T = 30°$C, $c_{\rm m} = 160$ mg/mL, Larmor frequency between 10 kHz and 110 MHz, $R_{1,\rm bulk} = 0.3$ s^{-1}, $N_{\rm s}/N$ is calculated from Eqs. (4a, b) and Eq. 15-SI (see Table 1). The surface fractal dimension $d_{\rm f}$ can be obtained from the literature from the solvent accessible surface area (SASA) as a function of the protein radii using the Lee-Richards algorithm.[42] The activation energy for the free diffusion of water is well known as $E_{\rm d} = 4.7$ kcal/mol. This value of $E_{\rm d}$ leads to the minimal activated energies $E_{\rm A,min} = 1$ kcal/mol and $E_{\rm A',min} = 0.6$ kcal/mol of the buried water molecules and their associated minimal values of the correlation times $\tau_{\rm min} = 12.2$ ps and $\tau'_{\rm min} = 6.3$ ps, respectively. Finally, we choose a small value for the equilibrium constant $K_{eq} = 4$ defined in Eq. 19-SI. (ii) The varied parameters are the two exponents $\alpha = 0.65$ and $\alpha' = 1.4$ of the Pareto distributions of correlation times. This is an extremely sensitive choice of the fits that fixes the values of the low frequency plateau and the slope of the power law at large frequency (see Fig. 6-SI). The remaining varied parameters are the activated energies of the buried water molecules in the two neighboring wells $E_{\rm A',max}$ for the "sse" events and $E_{\rm A',max}$ for the "dse" events. Values of $\tau'_{\rm max}$ are shown in the Table 1.

As expected, we found that the values of $\tau'_{\max}$ for the "dse" events are larger than the ones found for the "sse" events. This makes sense because the occurrence of the "dse" events is much lower than that of the "sse" events.

Fast surface relaxation modelling: (i) There are only two parameters for this relaxation process. The surface translational correlation time is fixed to the value $\tau_{\rm m} = 37$ ps that has been previously measured in ref.[27] This value corresponds to a water surface diffusion of $D_{\rm bulk}/3$. (ii) The correlation time of residence at the protein surface $\tau_{\rm s}$ that is varied through the dynamical surface parameter $A = \tau_{\rm s}/\tau_{\rm m}$. In fact, we vary $A_{\rm sse}$ and take $A_{\rm dse} = 4A_{\rm sse}$ because the surface residence time $\tau_{\rm s}$ follows the surface area of a protein of radius $2R_0$ which is 4 times the ones of a monomer unit.

We have considered "double protein surface exploration" (dse) for water molecules between proteins close to each other when the distance between neighbouring protein surfaces $\langle d \rangle$ is of the order of the individual protein radii (see the schematic diagrams in the insets of Fig. 3 and 2-SI). In this case, the correlation time $\tau'_{\max}$ is enlarged since the water molecules jump between two neighboring proteins. In the range of the highest protein concentrations ($c_{\rm m} \approx 160$ mg/mL), these water molecular jumps thus require some spatial ($\langle d \rangle$) and time ($\tau'_{\max}$) "correlations" between neighboring proteins. In the absence of these correlations, case of dilute solutions, the cut-off of the measurable correlation times would be the timescale of individual protein tumbling (around 6 ns for LZM and 56 ns for BSA without added salt). Previous works[23,43,44] have shown that increasing the concentration of proteins in solution not only slows down the tumbling but also causes the appearance of a weak additional slow relaxation for the protein rotation. The correlation time of this slow relaxation is of the order of µs in the concentration range of the sample examined in the present study.[44] In this case, the finite lifetime τ' of water molecules within the protein structure becomes the effective cut-off of the measurable water proton correlation times, as in the case of immobilized proteins. The origin of this additional slow rotational dynamics likely arises from anisotropic protein-protein interactions, especially the long-range electrostatic interactions between the

inhomogeneous surface charge distribution of the proteins.[23,43,44]

Table 1: R_1 fitting parameters for LZM (top) and BSA (bottom), corresponding to the theoretical curves in Figure 1. Note that $A_{\mathrm{dse}} = 4A_{\mathrm{sse}}$.

System		d_{f}	$R_{1,\mathrm{fast}}$	$R_{1,\mathrm{slow}}$		N_{surf}/N
			A_{sse}	$E'_{\mathrm{A,max}}$ (sse, dse) [kcal/mol]	τ'_{max} (sse, dse) [ns]	(sse, dse)
LZM	No salt	2.07	1000	5.9, 6.5	39, 106	0.18, 0.008
	NaCl	2.11	1200	6.1, 6.6	55, 125	0.19, 0.008
	NaI	2.16	3500	6.7, 7.2	148, 316	0.21, 0.009
BSA	No salt	2.38	10000	7.3, 7.4	385, 469	0.41, 0.004
	NaCl	2.34	5000	7.2, 7.3	316, 398	0.37, 0.004
	NaI	2.30	3000	7.1, 7.2	286, 338	0.34, 0.003

Discussion

Our experimental results and accompanying model curves are presented in Figure 1. The experimental data are successfully reproduced by a model inspired by previously published expressions of Korb *et al.*[31] and Grebenkov *et al.*[27] for the slow and fast surface relaxation processes, respectively. The overall model of the NMRD profiles allows to make a link between the salt added and the protein surface roughness, as seen by a water molecule present transiently at its surface (expressed here as a fractal dimension, d_{f}), and also the residence times of both the long-lived ("embedded") and fast-moving ("surface") water molecules. The results from the NMRD profile modelling are summarized in Table 1. In the sequence: No salt $\rightarrow$ NaCl $\rightarrow$ NaI, data for LZM show firstly, that the surface fractal dimension increases. This entails a larger protein surface available for the water molecules and thus a higher proportion of water molecules affected by it (higher N_{surf}/N). Secondly, concerning the "embedded" water molecules, the activation barrier and waiting time for jumps between different potential energy wells. For BSA along the same sequence, No salt $\rightarrow$ NaCl $\rightarrow$ NaI, all the above-mentioned parameters decrease in value.

The departure point for our understanding of these opposite trends is an assessment of the

initial condition, the "No salt" case. Let us consider the surface roughness of the two proteins, BSA and LZM, in this "bare" case, with no salt ions attached to their surface. Following the method of Lewis et al,[45,46] the surface roughness of each protein can be estimated on the basis of their PDB structures and the accessible surface area (ASA) for a probe of a given size exploring the entire surface. In our case, the probe of interest has the size of a water molecule (radius of 1.4 Å, the conventional value). Using Lewis' method, the surface fractal dimension of LZM is 2.04 while for BSA it is 2.34 (see SI p. 8 for details). These values are in an excellent agreement with the d_{f} values obtained from our model aiming to reproduce water dynamics: 2.07 and 2.38 for LZM and BSA respectively, see Table 1. Overall, the d_{f} values obtained by these two independent methods attest to the increased roughness of the "bare" BSA molecule in comparison to LZM.

When small molecules attach to a surface d_{f} changes its value, and this change can act in either direction.[47] A rougher protein surface can indeed bind more water molecules than a smooth surface, a factor of three was suggested in Ref.[48] Our modelling of the NMR relaxation profiles suggests that the initially smooth LZM surface becomes rougher as larger anions bind to its surface. On the contrary, the inherent roughness of the "bare" BSA surface decreases as larger anions bind to it. This is the central idea of our interpretation and is depicted pictorially in Figure 2. Further, a rougher surface slows down the dynamics of solvent molecules next to it.[49] This is reflected in our model via the residence times of both the long-lived ("embedded") and fast-moving ("surface") water molecules.

In favour of the above picture, in Figure 4 we present NMRD data for BSA as a function of salt concentration. The analogous data for LZM is shown in Figure 7-SI. R_1 increases with increasing NaCl concentration for LZM solutions as: 0.10 M NaCl > 0.05 M NaCl > 0.00 M NaCl. With increasing salt concentration more ions attach to the protein surface which results in a rougher surface and higher NMRD relaxation rate in LZM solutions. On the contrary, for BSA the addition of 0.05 M NaI causes an immediate decrease of R_1. The profile stays the same for all NaI concentrations between 0.05 M and 0.60 M. When

the concentration exceeds 0.60 M, R_1 begins to increase with salt concentration. In our picture, only after initial smoothing of the BSA surface, the surface becomes rougher with salt addition, as in the case of LZM.

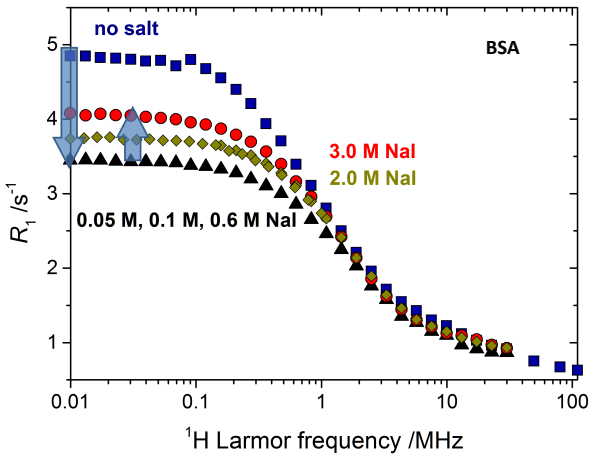

Figure 4: NMRD profiles of BSA solutions with several NaI concentrations: 0.05, 0.10 and 0.60 M NaI (black triangles), 2.0 M NaI (golden deltoids) and 3.0 M NaI (red circles). No added salt case is presented in blue squares. Arrow facing down represents an initial decrease of R_1 for low NaI concentrations (up to 0.60 M) and arrow facing up represents increase of R_1 for higher NaI concentrations. $T = 30$ °C and c_m=160 mg/mL.

As mentioned previously, effects of salt ions on surface water dynamics have been interpreted in the past by evoking the formation of protein oligomers, on solutions with salt concentration of 0.5-0.6 M, thus in a region where Debye-Hückel screening is essentially complete.[33,34] This study deals with a different phenomenon, as it reveals both an increase and a decrease in low-frequency R_1 values for protein solutions at a much lower salt concentration range, 0.05-0.1 M. Importantly, a decrease in low-frequency R_1 values cannot be accounted for by oligomer formation. Our previous dynamic light scattering study[37] confirms the absence of aggregates in BSA and LZM solutions, up to protein concentrations of 160 mg mL^{-1}, upon addition of 0.1 M salt, i.e. the low salt concentration regime of concern here. For comparison, the NMRD profile for an aggregated LZM solution is shown in Figure 8-SI, featuring no plateau in the low frequency regime and relaxation rates increased by more than one order of magnitude with respect to those in stable LZM solutions. For

non-aggregated solutions, our model predicts correctly the NMRD profiles as a function of protein concentration, as presented in Figure 9-SI.

Conclusion

The experimental data presented here show clearly contrasting salt effects in ^{1}H NMRD profiles of two different protein solutions. Our interpretation of this phenomenon is based on the variation of protein surface roughness, as seen by the water molecules present transiently at the protein surface. We have developed a theoretical model with several important features: (a) the multi-scale model accounts for the non-Lorentzian shape of the NMRD profiles by a superposition of a slow and a fast relaxation process, achieving to reproduce the experimental data over 4 decades in the Larmor frequency, 10 kHz to 110 MHz; (b) the model is applicable to a large protein concentration range, with a specific feature incorporating "single" and "double" surface exploration terms, necessary to reach the high protein concentration regime; (c) the model accounts for observed salt effects via a quantitative measure of the protein surface roughness, represented by the surface fractal dimension, and the water residence times of both the long-lived ("embedded") and fast-moving ("surface") water molecules at the protein surface. The response to the presence of salt ions at the surface of a protein is thus protein-specific, linked in our model to geometrical aspects of the individual protein surface. In our opinion, this is a key to understanding the specificity of ion-water-protein interactions. Thus, while the Hofmeister ordering serves as a first guide for predicting salt effects in protein, or macromolecular solutions in general, its universality across the different macromolecules and measured physical quantities is unlikely to be found.

Acknowledgement

The authors acknowledge the financial support of CNRS (PICS - Projet International de Coopération Scientifique), the P1-0201 and J1-1708 research grants of the Slovenian Research

Agency (ARRS) and the COST (European Cooperation in Science and Technology) Action CA15209 EURELAX (European Network on NMR Relaxometry). The authors are grateful for the access to the NMR relaxometry platform RELAXOME of the Institute of Materials of Paris (IMPC) funded by Région Ile de France, Sorbonne University and CNRS.

Supporting Information Available

An online supplement to this article can be found by visiting ACS Online. The Supporting Information includes: (i) Temperature dependence of NMR relaxation time, (ii) Dependence of inter-protein distance and water surface fraction on protein concentration, (iii) Longitudinal relaxation rate at low frequencies due to slow surface motions of water, (iv) Longitudinal relaxation rate at high frequencies due to the fast motions, (v) Modelling of protein surface roughness, (vi) Transient water fraction for single $(N_s/N)_{sse}$ and double $(N_s/N)_{dse}$ protein surface explorations, (vii) Overall longitudinal relaxation rate $R_1(\omega_0)$, (viii) SASA and protein roughness by Lewis' method, and (ix) Additional $R_1(\omega_0)$ profiles for LZM and BSA.

References

(1) Gunton, J. D.; Shiryayev, A.; Pagan, D. L. *Protein Condensation: Kinetic Pathways to Crystallization and Disease*; Cambridge University Press, 2007.

(2) Amin, S.; Barnett, G. V.; Pathak, J. A.; Roberts, C. J.; Sarangapani, P. S. Protein aggregation, particle formation, characterization & rheology. *Curr. Opinion Coll. Interface Sci.* **2014**, *19*, 438–449.

(3) Kastelic, M.; Kalyuzhnyi, Y. V.; Hribar-Lee, B.; Dill, K. A.; Vlachy, V. Protein aggregation in salt solutions. *Proc. Natl. Acad. Sci. USA* **2015**, *112*, 6766–6770.

(4) Chiti, F.; Dobson, C. M. Protein misfolding, functional amyloid, and human diseases. *Anu. Rev. Biochem.* **2006**, *75*, 333–366.

(5) Bye, J. W.; Platts, L.; Falconer, R. J. Biopharmaceutical liquid formulation: a review of the science of protein stability and solubility in aqueous environments. *Biotechnol. Lett.* **2014**, *36*, 869–875.

(6) Brown, G. Total cell protein-concentration as an evolutionary constraint on the metabolic control distribution in cells. *J. Theor. Biol.* **1991**, *153*, 195–203.

(7) Zimmerman, S.; Minton, A. Macromolecular crowding - biochemical, biophysical, and physiological consequences. *Annu. Rev. Biophys. Biomol. Struct.* **1993**, *22*, 27–65.

(8) Garidel, P.; Kuhn, A. B.; Schaefer, L. V.; Karow-Zwick, A. R.; Blech, M. High-concentration protein formulations: How high is high? *Eur. J. Pharm. Biopharm.* **2017**, *119*, 353–360.

(9) Zhang, Y.; Furyk, S.; Bergbreiter, D. E.; Cremer, P. S. Specific Ion Effects on the Water Solubility of Macromolecules: PNIPAM and the Hofmeister Series. *J. Am. Chem. Soc.* **2005**, *127*, 14505–14510.

(10) Zhang, Y.; Cremer, P. S. The inverse and direct Hofmeister series for lysozyme. *Proc. Natl. Acad. Sci. USA* **2009**, *106*, 15249–15253.

(11) Nostro, P. L.; Ninham, B. W. Hofmeister phenomena: An update on ion specificity in biology. *Chem. Rev.* **2012**, *112*, 2286–2322.

(12) W Kunz, Specific ion effects in colloidal and biological systems. *Curr. Opinion Coll. Interface Sci.* **2010**, *15*, 34–39.

(13) KD Collins, Why continuum electrostatics theories cannot explain biological structure, polyelectrolytes or ionic strength effects in ion-protein interactions. *Biophys. Chem.* **2012**, *167*, 43–59.

(14) A Salis, BW Ninham, Models and mechanisms of Hofmeister effects in electrolyte solutions, and colloid and protein systems revisited. *Chem. Soc. Rev.* **2014**, *43*, 7358.

(15) N Malikova, AL Rollet, S Čebašek, M Tomšič, V Vlachy, On the crossroads of current polyelectrolyte theory and counterion-specific effects. *Phys. Chem. Chem. Phys.* **2015**, *17*, 5650–5658.

(16) Bryant, R.; Shirley, W. Dynamical deductions from nuclear magnetic-resonance relaxation measurements at the water-protein interface. *Biophys. Journal* **1980**, *32*, 3–16.

(17) Ball, P. Water is an active matrix of life for cell and molecular biology. *Proc. Natl. Acad. Sci. USA* **2017**, *114*, 13327–13335.

(18) Kimmich, R., Ed. *Field-cycling NMR Relaxometry*; New Developments in NMR; The Royal Society of Chemistry, 2019; pp P001–571.

(19) Bryant, R. The dynamics of water-protein interactions. *Annu. Rev. Biophys. Biomol. Struct.* **1996**, *25*, 29–53.

(20) Halle, B.; Denisov, V. *Nuclear Magnetic Resonance Of Biological Macromolecules, Part A*; Methods In Enzymology A; 2001; Vol. 338; pp 178–201.

(21) Luchinat, C.; Parigi, G. Collective relaxation of protein protons at very low magnetic field: A new window on protein dynamics and aggregation. *J. Am. Chem. Soc.* **2007**, *129*, 1055–1064.

(22) G Parigi, N Rezaei-Ghaleh, A Giachetti, S Becker, C Fernandez, M Blackledge, C Griesinger, M Zweckstetter, C Luchinat, Long-Range Correlated Dynamics in Intrinsically Disordered Proteins. *J. Am. Chem. Soc.* **2014**, *136*, 16201–16209.

(23) M Roos, M Hofmann, S Link, M Ott, J Balbach, E Roessler, K Saalwaechter, A Krushelnitsky, The "long tail" of the protein tumbling correlation function: observation by 1H NMR relaxometry in a wide frequency and concentration range. *J. Biomol. NMR* **2015**, *63*, 403–415.

(24) Roos, M.; Link, S.; Balbach, J.; Krushelnitsky, A.; Saalwaechter, K. NMR-Detected Brownian Dynamics of alpha B-Crystallin over a Wide Range of Concentrations. *Biophys. Journal* **2015**, *108*, 98–106.

(25) Persson, E.; Halle, B. Nanosecond to microsecond protein dynamics probed by magnetic relaxation dispersion of buried water molecules. *J. Am. Chem. Soc.* **2008**, *130*, 1774–1787.

(26) Persson, F.; Halle, B. Transient Access to the Protein Interior: Simulation versus NMR. *J. Am. Chem. Soc.* **2013**, *135*, 8735–8748.

(27) Grebenkov, D. S.; Goddard, Y. A.; Diakova, G.; Korb, J. P.; Bryant, R. G. Dimensionality of diffusive exploration at the protein interface in solution. *J. Phys. Chem. B* **2009**, *113*, 13347–13356.

(28) Korb, J.-P. Multiscale nuclear magnetic relaxation dispersion of complex liquids in bulk and confinement. *Prog. Nucl. Magn. Reson. Spectrosc.* **2018**, *104*, 12–55.

(29) Huang, Y.; Nam, K.; Westlund, P.-O. The water R-1(omega) NMRD profiles of a hydrated protein from molecular dynamics simulation. *Phys. Chem. Chem. Phys.* **2013**, *15*, 14089–14097.

(30) Diakova, G.; Goddard, Y. A.; Korb, J.-P.; Bryant, R. G. Water and Backbone Dynamics in a Hydrated Protein. *Biophys. Journal* **2010**, *98*, 138–146.

(31) Korb, J.-P.; Goddard, Y.; Pajski, J.; Diakova, G.; Bryant, R. G. Extreme-Values Statistics and Dynamics of Water at Protein Interfaces. *J. Phys. Chem. B* **2011**, *115*, 12845–12858.

(32) Bryant, R. G. Dynamics of water in and around proteins characterized by H-1-spin-lattice relaxometry. *C. R. Phys.* **2010**, *11*, 128–135.

(33) Gottschalk, M.; Venu, K.; Halle, B. Protein Self-Association in Solution: The Bovine Pancreatic Trypsin Inhibitor Decamer. *Biophys. Journal* **2003**, *84*, 3941–3958.

(34) Gottschalk, M.; Nilsson, H.; Roos, H.; Halle, B. Protein self-association in solution: The bovine beta-lactoglobulin dimer and octamer. *Protein Sci.* **2003**, *12*, 2404–2411.

(35) Stanley, C. G.; von Hippel, P. H. Calculation of protein extinction coefficients from amino acid sequence data. *Anal. Biochem.* **1989**, *182*, 319–326.

(36) Wang, Y.; Annunziata, O. Comparison between protein-polyethylene glycol (PEG) interactions and the effect of PEG on protein-protein interactions using the liquid-liquid phase transition. *J. Phys. Chem. B* **2007**, *111*, 1222–1230.

(37) T Janc, M Lukšič, V Vlachy, B Rigaud, A.-L. Rollet, J.-P. Korb, G Mériguet, N Malikova, Ion-specificity and surface water dynamics in protein solutions. *Phys. Chem. Chem. Phys.* **2018**, *20*, 30340–30350.

(38) Luchinat, C.; Parigi, G.; Ravera, E. Water and Protein Dynamics in Sedimented Systems: A Relaxometric Investigation. *Chem. Phys. Chem.* **2013**, *14*, 3156–3161.

(39) Venu, K.; Denisov, V.; Halle, B. Water H-1 magnetic relaxation dispersion in protein solutions. A quantitative assessment of internal hydration, proton exchange, and cross-relaxation. *J. Am. Chem. Soc.* **1997**, *119*, 3122–3134.

(40) Parmar, A. S.; Muschol, M. Hydration and Hydrodynamic Interactions of Lysozyme: Effects of Chaotropic versus Kosmotropic Ions. *Biophys. J.* **2009**, *97*, 590–598.

(41) Dorshow, R.; Nicoli, D. F. The effect of hydrodynamics on the diffusivity of charged macromolecules: Application to BSA. *J. Chem. Phys.* **1981**, *75*, 5853–5856.

(42) Lee, B.; Richards, F. The interpretation of protein structures: Estimation of static accessibility. *J. Mol. Biol.* **1971**, *55*, 379–400.

(43) Roos, M.; Ott, M.; Hofmann, M.; Link, S.; Rössler, E.; Balbach, J.; Krushelnitsky, A.; Saalwächter, K. Coupling and Decoupling of Rotational and Translational Diffusion of Proteins under Crowding Conditions. *J. Am. Chem. Soc.* **2016**, *138*, 10365–10372.

(44) Krushelnitsky, A. Intermolecular electrostatic interactions and Brownian tumbling in protein solutions. *Phys. Chem. Chem. Phys.* **2006**, *8*, 2117.

(45) Lewis, M.; Rees, D. Fractal surfaces of proteins. *Science* **1985**, *230*, 1163–1165.

(46) Dewey, T. G. Protein structure and polymer collapse. *J. Chem. Phys.* **1993**, *98*, 2250–2257.

(47) Banerji, A.; Navare, C. Fractal nature of protein surface roughness: a note on quantification of change of surface roughness in active sites, before and after binding. *J. Mol. Recognit.* **2013**, *26*, 201–214.

(48) LA Kuhn, MA Siani, ME Pique, CL Fisher, ED Getzoff, JA Tainer, The Interdependence of Protein Surface Topography and Bound Water Molecules Revealed by Surface Accessibility and Fractal Density Measures. *J. Mol. Biol.* **1992**, *228*, 13–22.

(49) Choi, J.-H.; Lee, S. Correlation between the roughness degree of a protein surface and the mobility of solvent molecules on the surface. *J. Chem. Phys.* **2000**, *113*, 6326–6329.

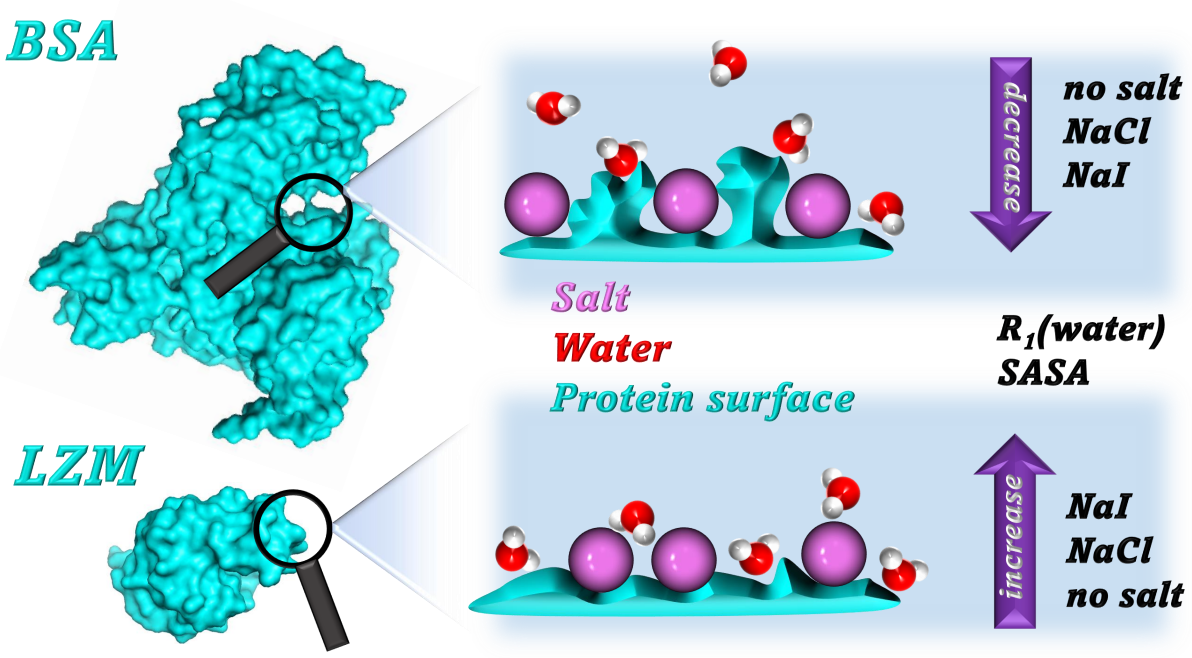

Figure 5: For Table of Contents Only